

Supplementary information

Performance and stability evaluation of LaF_3 thin film waveplates for high-power 266 nm laser applications

*Darija Astrauskyte, Mantas Slipkauskas, Saulius Tumenas, Aušra Selskiene, Lukas Ramalis, and Lina Grineviciute**

Supplementary 1. Autocorrelation analysis

The structural anisotropy of anisotropic single-layer coatings was analyzed using top-view SEM images and autocorrelation analysis¹ (Figure S1 a). Contour maps of the autocorrelation functions were obtained using MATLAB software (Figure S1 b). Cross-sections through the central region of the contour maps were extracted along the X and Y axes (Figure S1 c), and the structural anisotropy parameter k was calculated from ratio of the full widths at half maximum (FWHM) of both cross-sections. This analysis was performed for all single-layer anisotropic coatings.

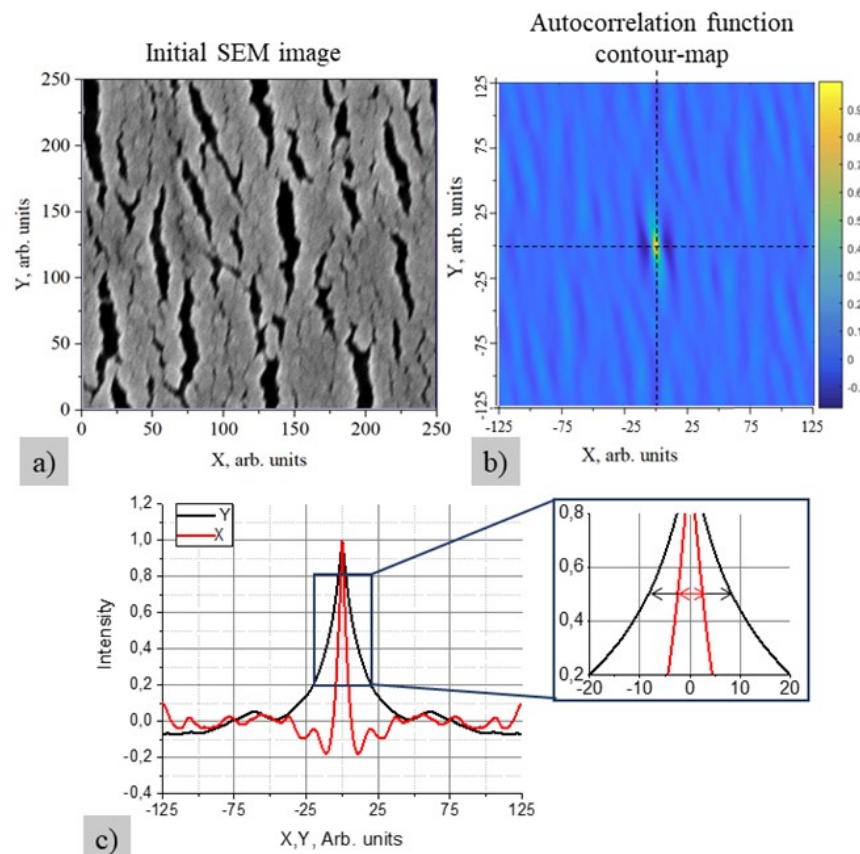


Figure S1. (a) Top-view SEM image of the anisotropic coating, (b) contour map of the autocorrelation function, and (c) cross-sections through the central region of the contour map along the X and Y axes (the inset shows the FWHM for the X and Y axis cross-sections).

Supplementary 2. Optical properties of dense single-layer LaF_3 coatings

To compare the performance of different evaporation techniques, dense LaF_3 single-layer coatings (300 nm thick) were deposited via EBE and thermal evaporation at a 0° deposition angle under constant substrate rotation. In addition, a thicker LaF_3 layer (1 μm thick) was produced via EBE to evaluate the effect of film thickness on optical losses. Transmittance and reflectance spectra of all samples were measured (Figure S2 a), and the effective refractive index dispersions were extracted from these spectra using OptiChar software (Figure S 2b). At a wavelength of 266 nm, the refractive indices of LaF_3 films prepared via EBE and thermal evaporation were 1.58 and 1.59, respectively, consistent with reported values in literature^{2,3}. Optical losses were lower for 300 nm thick EBE coating (0.07%), whereas the corresponding film produced via thermal evaporation showed higher losses of 0.49% (Figure S2 b). These results are consistent with the findings of Bischoff et al.⁴, who reported significantly greater optical losses in CaF_2 films produced via thermal evaporation compared to EBE. They attributed this to chemical reactions between the evaporating material and the molybdenum boat, producing MoF_x compounds that can introduce defects and increase UV absorption. In EBE process, the source material is locally heated, minimizing interaction with the crucible and thereby suppressing such reactions. Optical losses of 33.65% at 266 nm were observed for 1 μm thick EBE-deposited LaF_3 coating (Figure S2 b), attributed to cracking of the coating, probably caused by film stress (Figure S2 e). In contrast, thinner 300 nm thick coatings exhibited an undamaged surface (Figure S2 c and d).

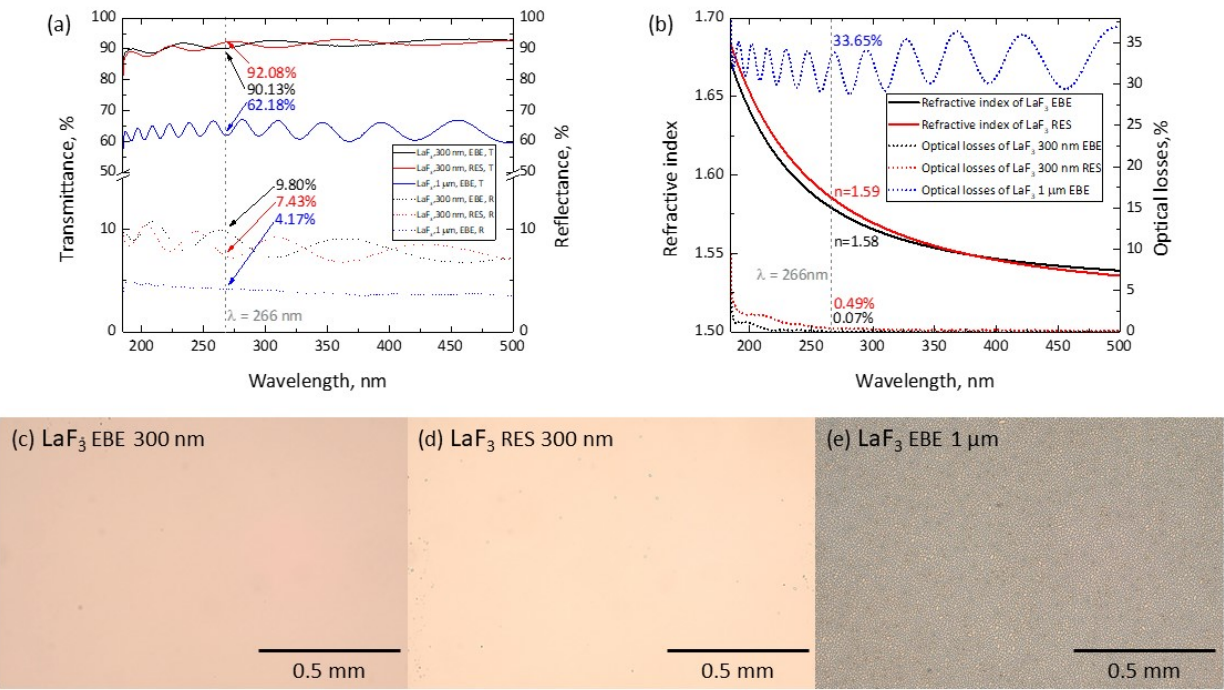


Figure S2. Optical properties of dense single-layer LaF_3 coatings: (a) transmittance and reflectance spectra, (b) dispersions of refractive indices and optical losses. Optical microscopy micrographs of: (c) 300 nm thick EBE-deposited LaF_3 film, (d) 300 nm thick thermally evaporated LaF_3 film, and (e) 1 μm thick EBE-deposited LaF_3 film.

Supplementary 3. XPS analysis of dense single-layer LaF_3 coatings

Furthermore, XPS analysis was employed to determine the chemical composition of 300 nm thick LaF_3 coatings and to evaluate the oxide formation, which can adversely affect the LIDT. Lanthanum oxides,

with a bandgap of 5.3 eV⁵, are expected to exhibit a lower LIDT than lanthanum fluorides, whose bandgap is 9.4 eV⁶. XPS analysis revealed that both thermally evaporated and EB evaporated films contained a minor fraction of lanthanum oxides. Based on XPS spectral peak analysis, the EBE-deposited LaF₃ coating consisted of La4d (24.29%), F1s (67.44%), and O1s (8.26%), corresponding to a LaF₃/LaO ratio of 2.41 (Figure S3 a). In comparison, the thermally evaporated LaF₃ film contained La4d (24.99%), F1s (67.72%), and O1s (7.29%), yielding a LaF₃/LaO ratio of 2.85 (Figure S3 b). Oxygen incorporation in LaF₃ films is attributed to residual gases in the vacuum chamber during deposition, as well as post-deposition exposure to the ambient conditions.

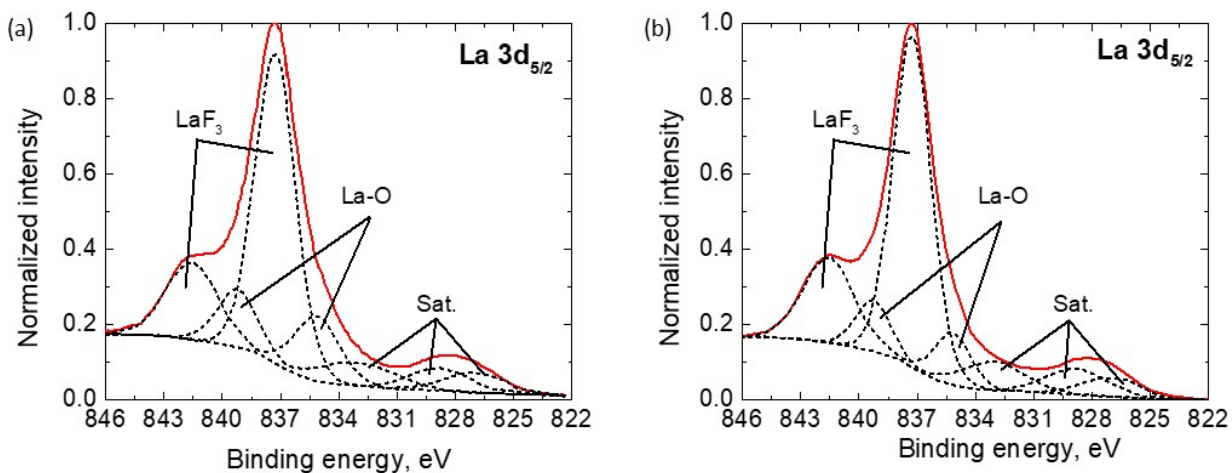


Figure S3. XPS spectra of dense single-layer LaF₃ films deposited by (a) electron beam evaporation and (b) thermal evaporation.

Supplementary 4. Defect density of anisotropic single-layer LaF₃ coatings

Since high defect density can reduce the LIDT and increase scattering losses, the defect density of the anisotropic LaF₃ coatings was evaluated using dark-field optical microscopy (Olympus BX41 optical microscope). Dark-field imaging was chosen because it enhances the contrast of small-scale surface features by collecting only light scattered from defects. For each sample, the surface was scanned using 5x magnification, acquiring 117 micrographs to obtain a complete spatial map (unprocessed images are shown in Figure S4 a). The images were subsequently inverted and analyzed using ImageJ software (processed images are presented in Figure S4 b). Increasing the deposition angle from 60° to 80° increased the defect density, from 1.79 defects/nm² to 20.31 defects/nm². This can be attributed to enhanced coalescence of the columns into larger disordered features at higher deposition angles, which promotes defect formation.

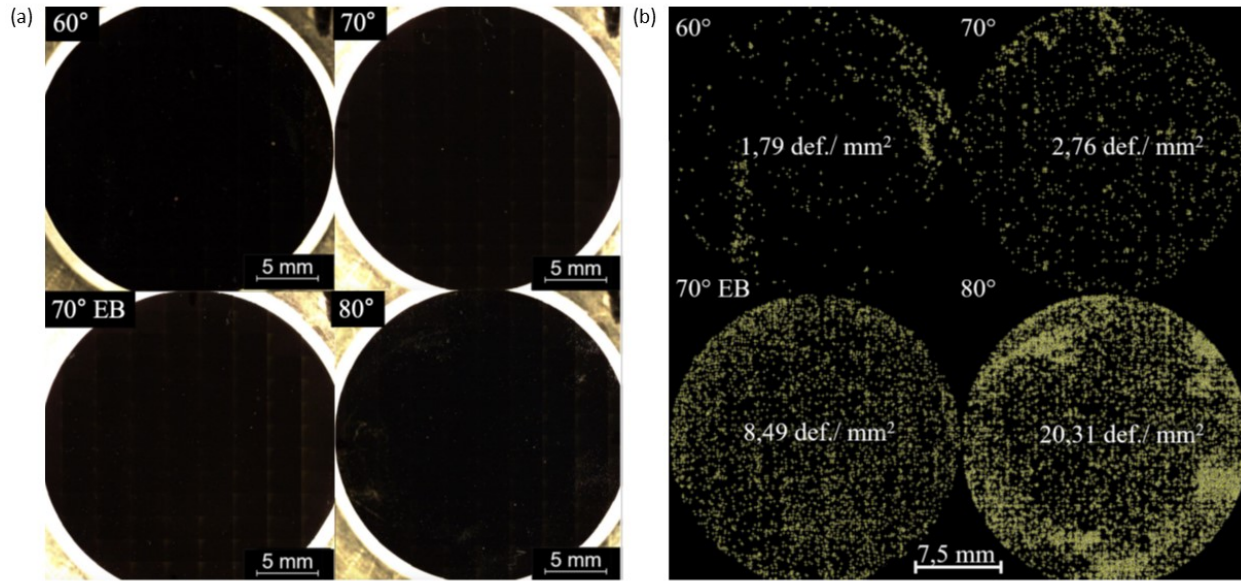


Figure S4. Defect density analysis of anisotropic single-layer LaF_3 coatings: (a) unprocessed images of the samples and (b) processed images of the samples used for defect density calculations.

In contrast, the coating deposited via EBE at a 70° deposition angle exhibited approximately three times higher defect density than the film deposited via thermal evaporation at the same angle. Such defect density in EBE-deposited films may result from random bursts of material ejected toward the substrate during the evaporation process, leading to the incorporation of larger particles and surface defects. In thermal evaporation, such effects are mitigated by a protective cover with apertures positioned above the source material, which reduces the deposition of large ejected particles onto the substrate.

References

- 1 C. Robertson, *J. Biomed. Opt.*, 2012, **17**, 080801.
- 2 L. V. Rodríguez-de Marcos, J. I. Larruquert, J. A. Méndez and J. A. Aznárez, *Opt. Mater. Express*, 2017, **7**, 989.
- 3 G. Liu, H. Yu, W. Zhang, Y. Jin, H. He and Z. Fan, *Thin Solid Films*, 2011, **519**, 3487–3491.
- 4 M. Bischoff, D. Gäbler, N. Kaiser, A. Chuvilin, U. Kaiser and A. Tünnermann, *Appl. Opt.*, 2008, **47**, C157.
- 5 Y. Zhao, K. Kita, K. Kyuno and A. Toriumi, *Applied Physics Letters*, 2009, **94**, 042901.
- 6 W. Pong and C. S. Inouye, *J. Opt. Soc. Am.*, 1978, **68**, 521.